*Int. J. Electrochem. Sci.*, 14 **(2019)** 453 – 469, doi: 10.20964/2019.01.22

International Journal of
ELECTROCHEMICAL
SCIENCE
www.electrochemsci.org

# Kinetic Study of Redox Probes on Glassy Carbon Electrode Functionalized by 4-nitrobenzene Diazonium

*William Richard, David Evrard*[*]*, Pierre Gros*

Laboratoire de Génie Chimique, Université de Toulouse, CNRS, INPT, UPS, Toulouse, France
[*]E-mail: evrard@chimie.ups-tlse.fr

*Received:* 23 July 2018 / *Accepted:* 22 August 2018 / *Published:* 30 November 2018

The electrochemical behavior of organic films grafted onto glassy carbon (GC) and bearing $NO_2$, NHOH or $NH_2$ groups was studied by using three different redox probes, namely ferricyanide $Fe(CN)_6^{3-}$, hexaammineruthenium(III) $Ru(NH_3)_6^{3+}$ and ferrocenemethanol FcMeOH. Films were prepared by grafting 4-nitrobenzene diazonium onto the GC surface by constant potential electrolysis for durations varying from 1 to 300 s. $NO_2$ groups were converted into NHOH and $NH_2$ by performing further electrolyses at the corresponding potentials. The redox probes were chosen because of their different global charge and electron transfer process. For all the as-obtained films, the Koutecky-Levich treatment was applied and the cathodic (β) and anodic (α) transfer coefficients were extracted. All these data were discussed and compared in order to better understand the structure and the electrochemical properties of the organic films.

**Keywords:** 4-nitrobenzene diazonium; electrode functionalization; stratified film; Koutecky-Levich analysis; electrochemical kinetics; redox probes

## 1. INTRODUCTION

Electrode surface functionalization has attracted tremendous attention in the last decades. Many strategies have been developed to purposely modify the electrode, such as self-assembled monolayers "SAMs" [1], conducting polymers [2] or nanoscale-based materials [3]. Amongst all these strategies dedicated to surface modification, electrografting is certainly the most studied one since it affords an easy, covalent way to immobilize additional functional groups of interest on the electrode [4]. This is particularly true considering diazonium compounds, since their versatility offers a wide range of potentialities [4-6]. Depending on the functional group borne by the aromatic skeleton, diazoniums have been used in many research fields such as molecular electronics [5], energy conversion and storage [7,8] and chemical [9,10] or biological [11,12] sensing. Further functionalization can also be achieved by

coupling chemical reactions to diazonium grafting, such as amine/carboxyl condensation [13], click chemistry [13,14] or electropolymerization in the case of conjugated monomer-functionalized diazonium [6,9,15]. The as-obtained mixed organic layers have been recently reviewed [16].

Because commercially available and bearing an electroactive nitro group, 4-nitrobenzene diazonium (NBD) has been used for many applications. Indeed, it served as a redox probe to evidence the difference of reactivity between single and multilayer graphene sheets [17], to highlight the effect of a radical scavenger on the organic layer formation [18], or to illustrate carbon surface nanopatterning [19]. Also, NBD was used to promote the covalent immobilization of organometallic model of enzyme onto carbon surface [20] or to modify the electrical properties of graphene field-effect transistors [21]. Thus, as so commonly used with various goals, NBD grafting and reduction mechanism was expected to be well-known for years. However, we have recently demonstrated that, contrary to what many authors claimed [22-27], NBD grafting onto the electrode surface and nitro groups reduction were definitely separated processes [28] and that the grafting step actually occurs at much higher potential than usually reported values, ca. 0.3 V vs. saturated calomel electrode (SCE), in accordance with the suggestion made earlier by Cline et al. [29]. Thus arose the possibility to afford an interface bearing only nitro groups, these latter being available for further electrochemical treatment. Indeed, it is well established that $NO_2$ can be reversibly converted into the corresponding radical anion in aprotic conditions [30], whereas in protic media the reduction mechanism is more complex, leading to $NH_2$ groups as final product through an intermediary, reversible redox couple, namely nitroso/hydroxylamine (NO/NHOH) [25,28]. In a recent work [31], we have showed by a coupled electrochemical and spectroscopic approach that reduction at -0.1 V vs. SCE of a NBD-functionalized glassy carbon (GC) electrode in aqueous solution leads to a stratified organic film in which the easier $NO_2$ moieties to be reduced are the closest ones to the electrode surface, and the last to be reduced are the ones located at the interface between the film and the solution. Thus, during the electrolysis, the organic film successively exhibits $NH_2$ groups at the electrode surface, then NHOH in its inner, intermediary part and finally remaining $NO_2$ at its outer interface. Only another electrolysis at potential as cathodic as -0.8 V vs. SCE allows a complete reduction of all electroactive groups into $NH_2$. Furthermore, we have also demonstrated that during electrolysis at -0.1 V the whole reaction rate is actually limited by the charge transfer process and that consequently there is no limitation from a lack of solvation, contrary to what was suggested by Ceccato et al. [32].

In this work, we present the study of GC electrodes functionalized by NBD, with the organic film bearing mainly or exclusively $NO_2$, NHOH or $NH_2$ moieties. In order to better characterize the organic layer and its structure, films with different thicknesses were prepared by varying NBD grafting time, and successively studied by means of several redox probes, namely ferricyanide $Fe(CN)_6^{3-}$, hexaammineruthenium(III) $Ru(NH_3)_6^{3+}$ and ferrocenemethanol FcMeOH. These latter were chosen because they present differences in their global charge (anionic, cationic or neutral, respectively) and electron transfer process (inner-sphere for ferricyanide, outer-sphere for the other two probes), and are thus expected to afford different electrochemical responses and behaviors [33]. For each probe and each film-functionalized GC electrode, steady-state voltammograms were recorded and the Koutecky-Levich mathematical treatment applied in order the cathodic ($\beta$) and anodic ($\alpha$) transfer coefficients to be extracted.

## 2. EXPERIMENTAL

### *2.1. Chemicals*

All products were used as received. 4-nitrobenzene diazonium (NBD) tetrafluoroborate ($C_6H_4N_3O_2BF_4$, 97 %) and ferricyanide(III) potassium ($K_3Fe(CN)_6$, 99 % powder) were purchased from Sigma-Aldrich. Aniline ($C_6H_4(NH_2)_2$ 99 %) was obtained from Fluka. Hexaammineruthenium(III) chloride ($Ru(NH_3)_6Cl_3$) and potassium hexafluorophosphate ($KPF_6$, 98 %) were purchased from Alfa Aesar. Potassium dihydrogenophosphate ($KH_2PO_4$), di-potassium hydrogenophosphate ($K_2PHO_4$) and hydroxymethylferrocene (Ferrocenemethanol FcMeOH, 97 %) were supplied by Acros Organics. Acid solutions were prepared by dilution of hydrochloric acid (37 % HCl) from VWR using Milli-Q water (18 MΩ cm), and were deaerated by bubbling Nitrogen during 10 minutes. A gas stream was maintained over the solutions during experiments.

### *2.2. Apparatus*

All electrochemical experiments were performed at room temperature using a Metrohm µ-Autolab II potentiostat interfaced to a personal computer and controlled with NOVA 1.11 software package. A classical three-electrode glass cell was used with a Metrohm platinum rod and a Radiometer saturated calomel electrode (SCE) connected to the cell by a capillary as counter and reference electrode, respectively. Working electrode was a 3 mm diameter glassy carbon (GC) rotating disk electrode from Radiometer.

### *2.3. Electrode functionalization*

Prior to modification, GC electrode was manually polished to a mirror-like finish successively with 9 µm, 3 µm and 1 µm diamond powder. After each step, the electrode was thoroughly rinsed with Milli-Q water and sonicated in ethanol for 5 min in order to remove any impurity.

Aniline was converted into phenyldiazonium by using a procedure previously reported for the synthesis of other diazonium compounds [14,34].

Freshly polished electrode was modified by constant potential electrolysis at 0.3 V in a 0.1 M HCl (pH 1) solution containing 2.5 mM NBD or phenyldiazonium for a given time ranging from 1 to 300 s. After modification, the electrode (designated as GC-$NO_2^{\text{grafting time}}$ or GC-$Ph^{\text{grafting time}}$, respectively) was carefully rinsed with Milli-Q water before and after sonication in ethanol during 5 minutes to remove weakly adsorbed moieties. Further modification was operated on GC-$NO_2^{\text{grafting time}}$ by successive constant potential electrolyses at -0.1 V and -0.8 V during 300 s in 0.1 M HCl to afford GC-$NHOH^{\text{grafting time}}$ and GC-$NH_2^{\text{grafting time}}$, respectively.

## 3. RESULTS AND DISCUSSION

### *3.1. Electrode functionalization*

Figure 1 presents the cyclic voltammograms (CVs) obtained on a carefully polished glassy carbon (GC) electrode dipped in a 0.1 M HCl solution containing 2.5 mM NBD. The shape of the first and second scans was classical and consistent with our previous reports [28,31]. Hence, Peak I observed on the first forward scan actually corresponded to diazonium reduction and subsequent grafting onto GC surface while Peaks II and III were rather related to $NO_2$ reduction in NHOH and $NH_2$ groups (Scheme 1).

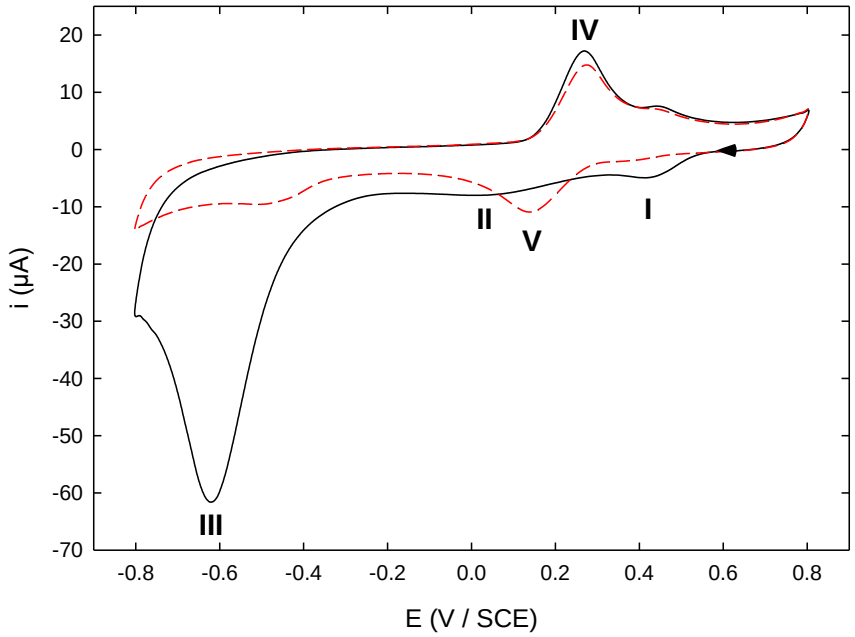


**Figure 1.** CV recorded in a 0.1 M HCl solution containing 2.5 mM NBD on a freshly polished GC electrode. (Solid line) first and (dashed line) second scan. Scan rate: 100 mV $s^{-1}$.

On the first backward scan, Peak IV was indicative of the presence of the NO/NHOH reversible redox system, together with Peak V on the second forward scan. It is worth noting that, on this latter scan, Peak I was no longer observed, in accordance with the self-inhibiting and blocking properties of diazonium layers [24,26]. In recent papers [28,31], we have proved that NBD grafting by constant potential electrolysis at a potential corresponding to Peak I (ca. 0.3 V) left the nitro groups unaffected by the electrochemical process. We have also demonstrated that reduction of the grafted layer at a potential close to that of Peak II afforded a stratified film bearing successively $NH_2$, NHOH and unaffected $NO_2$ while increasing the distance to the electrode surface, in accordance with a charge transfer-limited mechanism and an electron tunneling process, the efficiency of which decreases throughout the film from the electrode to the solution [31]. Further electrolysis at potential of Peak III finally led to a layer mainly consisting of $NH_2$ groups. For convenience, functionalized electrodes obtained by constant potential electrolysis at potential corresponding to Peak I, II or III were designated

as GC-$NO_2^{\text{grafting time}}$, GC-$NHOH^{\text{grafting time}}$ and GC-$NH_2^{\text{grafting time}}$, respectively (See Experimental Section for details).

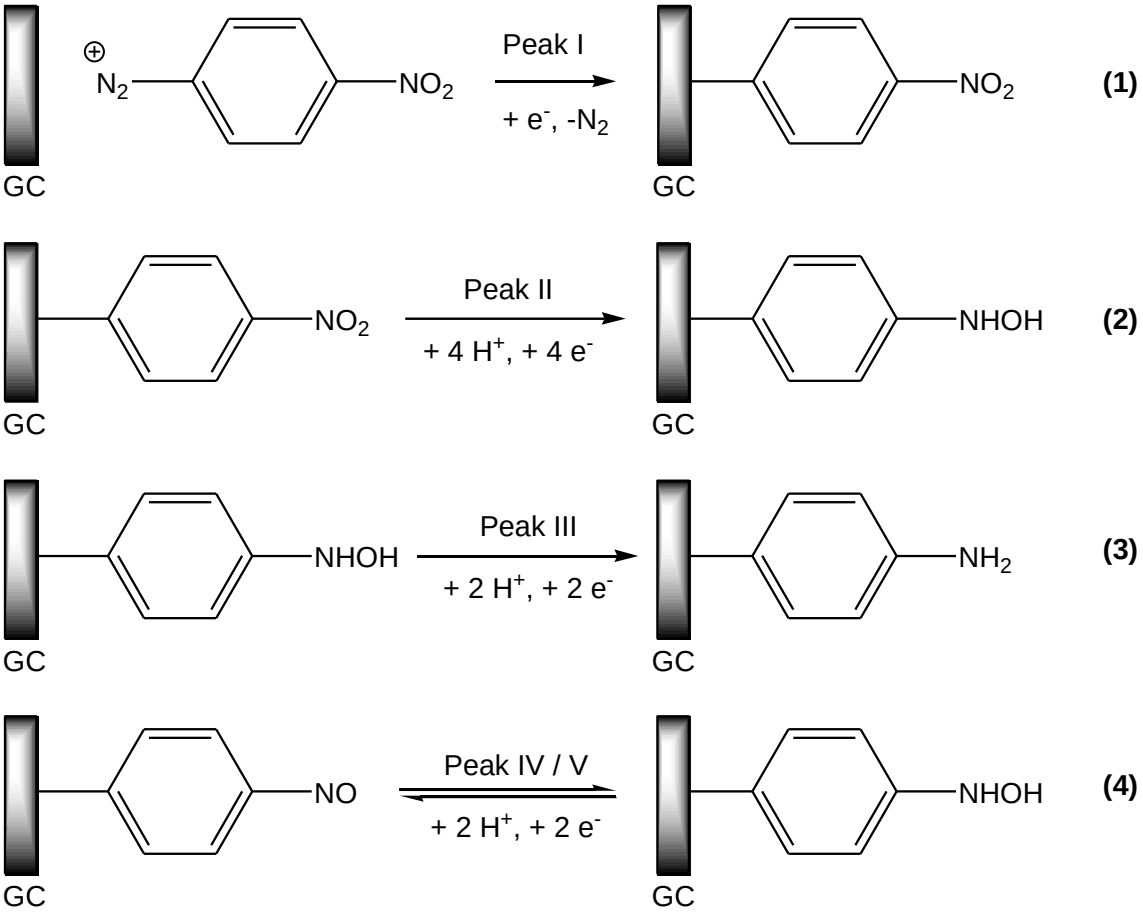


**Scheme 1.** Electrochemical reduction pathway of diazonium and $NO_2$ groups from NBD.

*3.2. Redox probes behavior at the functionalized electrodes*

Three different redox probes were chosen considering both their electrochemical behavior and their global charge, namely ferricyanide $Fe(CN)_6^{3-}$, hexaammineruthenium(III) $Ru(NH_3)_6^{3+}$ and ferrocenemethanol FcMeOH. Figure 2A shows the CVs obtained in a 0.1 M $KPF_6$ (pH 3.5) solution containing 5 mM $Fe(CN)_6^{3-}$ on bare GC and on the 3 different functionalized electrodes. On bare GC, $Fe(CN)_6^{3-}$ exhibited a quasireversible system with a $\Delta E_p$ = 210 mV consistent with many previous reports [22,33,35-37]. On GC-$NO_2^{300\ s}$, the reversible signal was almost totally suppressed, in accordance with the barrier effect of the organic layer [24,33].

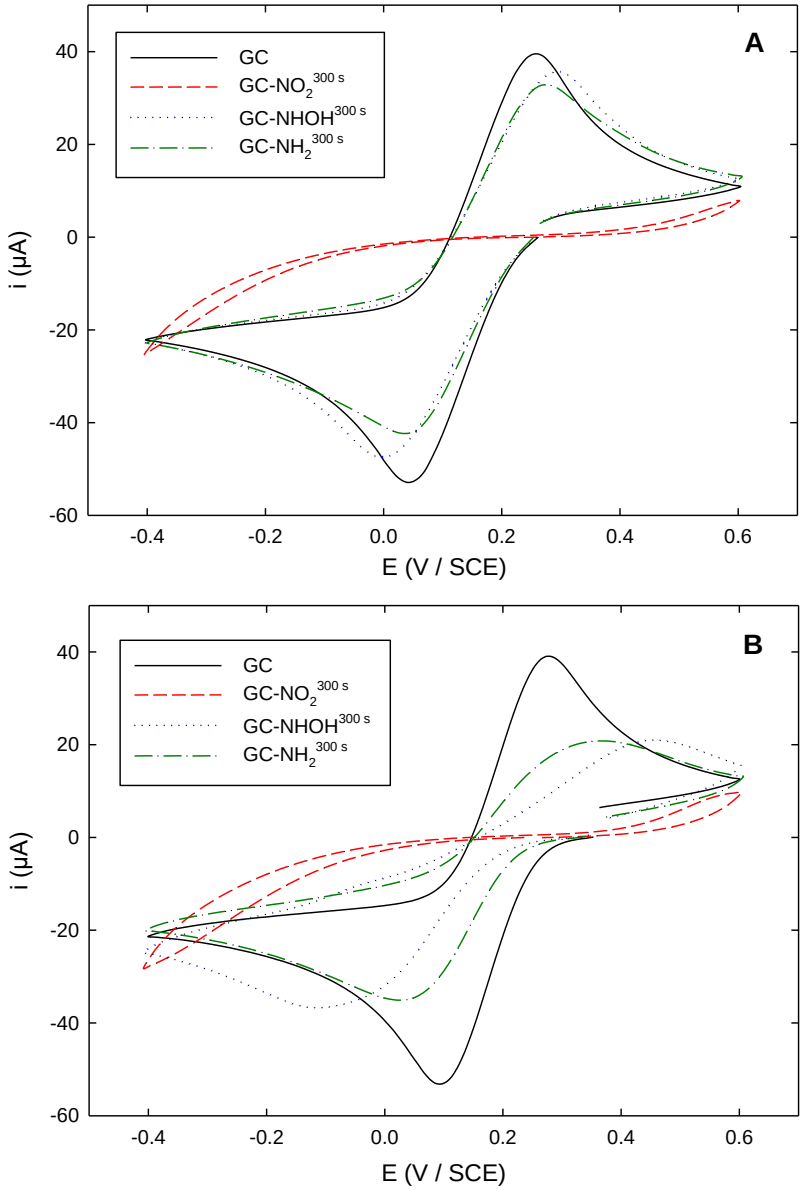


**Figure 2.** Cyclic voltammograms of 5 mM $Fe(CN)_6^{3-}$ recorded in (A) 0.1 M $KPF_6$ solution (pH 3.5) and (B) 0.1 M PBS solution (pH 7) on: (black solid line) unmodified GC; (red dashed line) GC-$NO_2^{300\ s}$; (blue dotted line) GC-$NHOH^{300\ s}$; (green dashed-dotted line) GC-$NH_2^{300\ s}$. Scan rate: 100 mV $s^{-1}$.

Indeed, the fact that the electrochemical signals were suppressed on GC-$NO_2^{300\ s}$ can be accounted for considering that the nitro-bearing layer is hydrophobic whereas $Fe(CN)_6^{3-}$ is rather hydrophilic [33,38]. Moreover, electrostatic repulsion may be also invoked between the electron-withdrawing $NO_2$ and the negatively charged redox probe. When GC-$NO_2^{300\ s}$ was changed to GC-$NHOH^{300\ s}$, the redox system was restored with a $\Delta E_p$ slightly larger (ca. 300 mV) than on bare GC, the peak currents being around 92 % of the initial signal. However, it has to be noticed that the observed signal contained a contribution from the NO/NHOH couple, the apparent standard potential of which being 0.15 V at such pH conditions [28]. On the basis of CVs recorded on the same electrode dipped in a redox probe-free $KPF_6$ solution (not shown), this contribution was evaluated around 10 % of the whole

electrochemical signal. The $Fe(CN)_6^{3-}$ redox system being known to proceed essentially via an inner-sphere mechanism [39,40], the signal recorded on GC-$NHOH^{300\ s}$ suggested the film to exhibit pinholes [33] or discontinuities [41]. Also, the thickness of the outer layer bearing the remaining $NO_2$ groups has to be very low, in order the approach of the redox probe not to be disfavored. Finally, a behavior similar to that observed on GC-$NHOH^{300\ s}$ was recorded on GC-$NH_2^{300\ s}$. The anodic and cathodic peak currents were however slightly lower than that previously observed on GC-$NHOH^{300\ s}$, mainly as a consequence of the absence of the NO/NHOH couple contribution.

The influence of pH value on the CVs was checked by performing the same experiment in a 0.1 M phosphate buffer saline (PBS) solution (pH 7) (Figure 2B). In such conditions, the behavior of $Fe(CN)_6^{3-}$ on GC-$NO_2^{300\ s}$ was similar to that obtained in $KPF_6$ (pH 3.5), i.e. the electrochemical signal was almost totally suppressed. On the contrary, on the other two functionalized electrodes, the redox signals were drastically different. Indeed, a slowed system was observed, with large peaks the current of which was only around 60 % of that recorded on bare GC and $\Delta E_p$ of 560 and 340 mV for GC-$NHOH^{300\ s}$ and GC-$NH_2^{300\ s}$, respectively. Thus, electrostatic interactions proved to be a key feature in $Fe(CN)_6^{3-}$ response on GC-$NHOH^{300\ s}$ and GC-$NH_2^{300\ s}$, both terminal groups being unprotonated at pH 7. Such a variation in $Fe(CN)_6^{3-}$ electrochemical response with respect to pH has already been reported by Schauff et al. in the case of a GC electrode functionalized with 4-diazo-*N*,*N*-diethylaniline [40]. Moreover, the important difference in the $\Delta E_p$ values recorded between GC-$NHOH^{300\ s}$ and GC-$NH_2^{300\ s}$ (ca. 560 mV and 340 mV, respectively) suggested steric hindrance effects to occur, thus favoring the hypothesis of an organic film exhibiting pinholes rather than discontinuities. The higher electron density on the NHOH groups compared to $NH_2$ groups may also account for the larger $\Delta E_p$ observed on GC-$NHOH^{300\ s}$.

The behavior of $Ru(NH_3)_6^{3+}$ on bare GC and on the three different functionalized interfaces was then examined. Figure 3A depicts the corresponding CVs obtained in 0.1 M $KPF_6$ (pH 3.5). On bare GC, the well-known reversible system for Ru(III)/Ru(II) was observed at -0.18 V, with a $\Delta E_p$ of 100 mV. GC-$NO_2^{300\ s}$ and GC-$NHOH^{300\ s}$ electrodes afforded very similar signals, the cathodic peak currents of which were almost comparable to that recorded on bare GC on the forward scan, with a slightly larger $\Delta E_p$ indicative of a slowed electron transfer kinetic. It is worth noting that the small reversible system observed on GC-$NHOH^{300\ s}$ at 0.15 V corresponded to the NO/NHOH couple as previously discussed. GC-$NH_2^{300\ s}$ also exhibited a slowed redox system, but in this latter case the cathodic peak current was significantly lower (around 35 %) than that recorded on bare GC. This may be indicative of a higher electrostatic repulsion between the cationic redox probe and the protonated form of the amino group. All these results were consistent with the outer-sphere mechanism attributed to the $Ru(NH_3)_6^{3+}$ redox system [22,39], inducing the probe is barely affected by the organic film at the electrode surface. It has to be noticed that the reoxidation peak on the backward scan was significantly smaller than the reduction one due to the fact that the potential was reversed at -0.4 V, i.e. close to the reduction peak potential, in order not to reach a potential value low enough to undergo the reduction of the organic layer into $NH_2$.

The same voltammograms recorded on the 4 different electrodes in 0.1 M PBS (pH 7) showed similar results (Figure 3B): whatever the functionalization operated on the electrode, the redox system was slowed compared to bare GC. However, in this case the absence of protonated NHOH or $NH_2$ groups was favorable to the cationic redox probe approach, from the electrostatic point of view, and consequently the recorded signals were better defined than those observed at pH 3.5.

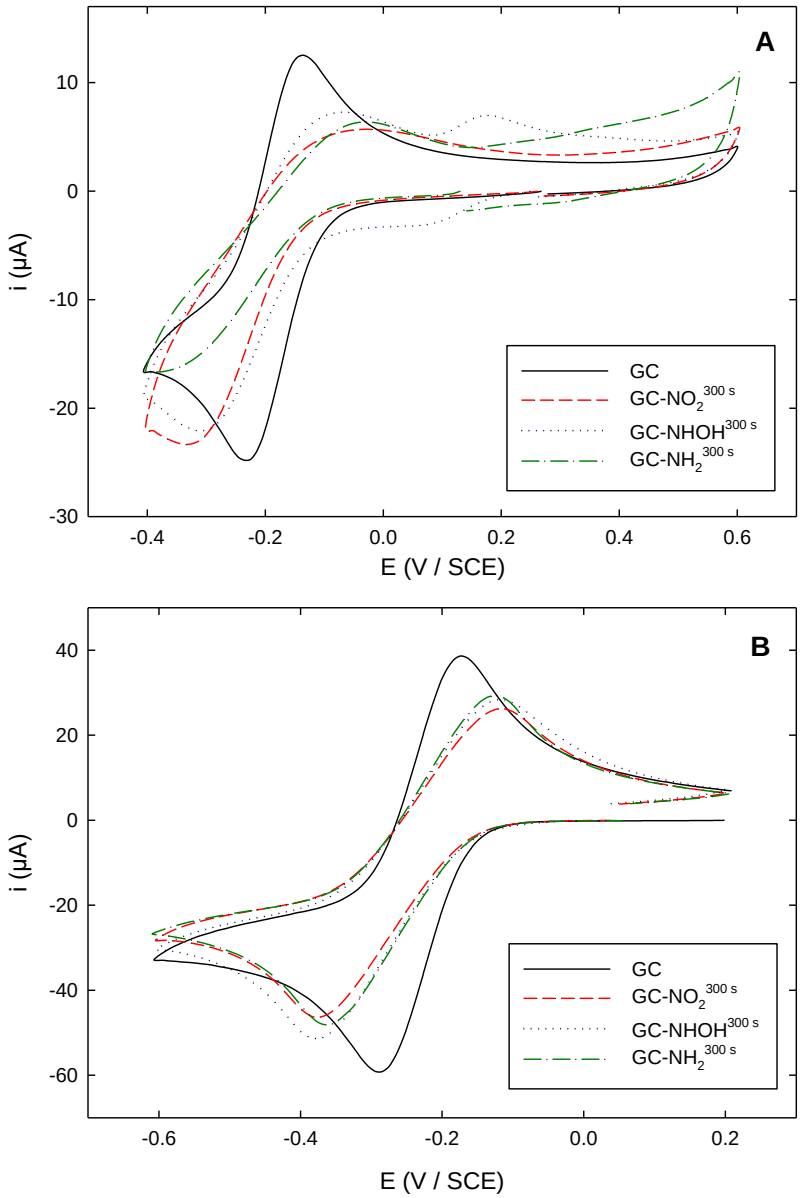


**Figure 3.** Cyclic voltammograms of 5 mM $Ru(NH_3)_6^{3+}$ recorded in (A) 0.1 M $KPF_6$ solution (pH 3.5) and (B) 0.1 M PBS solution (pH 7) on: (black solid line) unmodified GC; (red dashed line) GC-$NO_2^{300\ s}$; (blue dotted line) GC-$NHOH^{300\ s}$; (green dashed-dotted line) GC-$NH_2^{300\ s}$. Scan rate: 100 mV $s^{-1}$.

Finally, the response of the 4 different interfaces towards the neutral, outer-sphere mechanism FcMeOH probe was studied. Figure 4 depicts the results obtained in 0.1 M $KPF_6$ (pH 3.5). For all three functionalized interfaces, the reversible signal was only slightly slowed compared to bare GC, whatever the group borne by the film. The reduction peaks were smaller and larger than the oxidation ones, in accordance with a repulsive effect of the layer toward the ferrocenium cation.

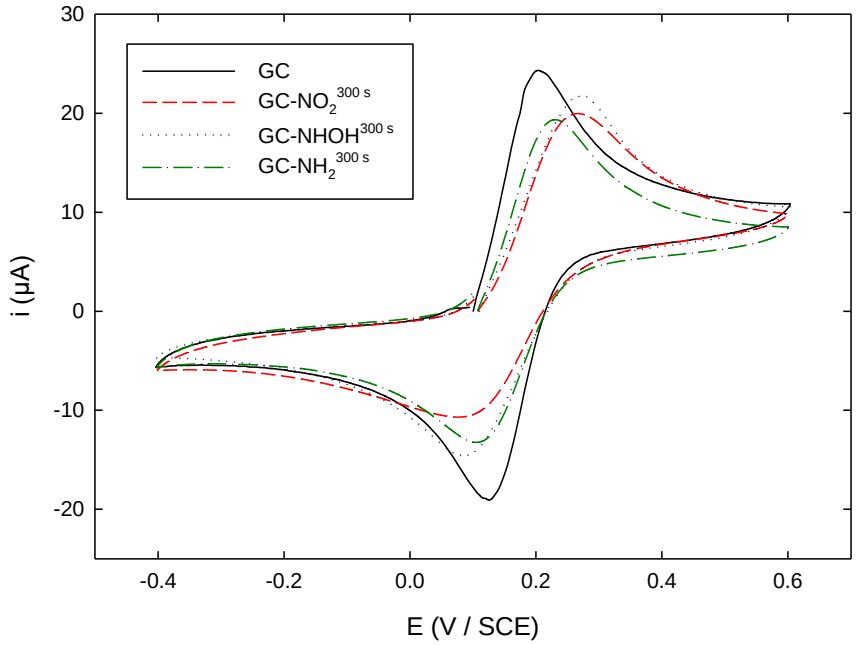


**Figure 4.** Cyclic voltammograms recorded in a 0.1 M $KPF_6$ solution (pH 3.5) containing 5 mM FcMeOH on: (black solid line) unmodified GC; (red dashed line) GC-$NO_2^{300\ s}$; (blue dotted line) GC-$NHOH^{300\ s}$; (green dashed-dotted line) GC-$NH_2^{300\ s}$. Scan rate: 100 mV $s^{-1}$.

### *3.3. Kinetics features of the redox probes at the functionalized electrodes*

In order to get more information upon kinetics features of the redox probes on the different modified electrode surface, a more systematic study was conducted. Figure 5 shows steady-state, linear voltammograms recorded at different rotation rates ω on GC-$NHOH^{300\ s}$ in 0.1 M $KPF_6$ (pH 3.5) containing 5 mM $Fe(CN)_6^{3-}$.

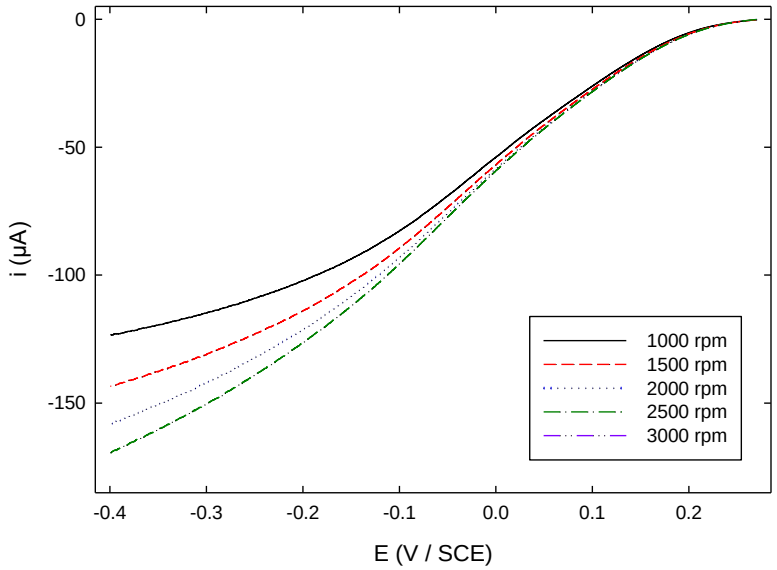


**Figure 5.** Steady-state voltammograms recorded in a 0.1 M $KPF_6$ solution (pH 3.5) containing 5 mM $Fe(CN)_6^{3-}$ on GC-$NHOH^{300\ s}$ at 5 mV $s^{-1}$ using different rotation rates ω.

Starting from the open-circuit potential value, the currents recorded were almost the same in the first part of the curve whatever the considered value of ω, in agreement with a charge transfer-limited reaction rate. Then the currents began to differ ones from the others while changing ω, as a consequence of mass transport limitation. It was verified that the current plateau evolved linearly as a function of the square root of the rotation rate ω (not shown). This result was consistent with the fact that the organic film was thin enough (ca. 4 nm [34]) in order not to hamper the diffusion process of the redox probe. Although the current plateau was not well-defined, the recorded data were treated using the Koutecky-Levich equation (Eq. (1)) [42]:

$$\frac{1}{i} = \frac{1}{i_k} + \frac{1}{i_d} = -\frac{1}{n\,F\,A\,k\,c} - \frac{1}{0.62\,n\,F\,A\,D^{2/3}\,\omega^{1/2}\,\nu^{-1/6}\,c} \qquad (1)$$

where $i_k$ and $i_d$ represent the kinetic limited and mass transfer controlled currents, respectively, A is the electrode active surface area (here assumed to be the geometrical area of the GC electrode, ca. $7.1\times10^{-2}$ $cm^2$), F is the Faraday constant (96500 C $mol^{-1}$), k is the potential-dependent charge transfer rate constant, c is $Fe(CN)_6^{3-}$ bulk concentration (5 mM), D is its diffusion coefficient ($5.5\times10^{-6}$ $cm^2$ $s^{-1}$) [43], and ν is the kinematic viscosity of the aqueous solution (0.01 $cm^2$ $s^{-1}$). According to Equation (1), the graph $i^{-1}$ as a function of $\omega^{-1/2}$ was plotted for potential values ranging from 0 to -0.4 V (Figure 6).

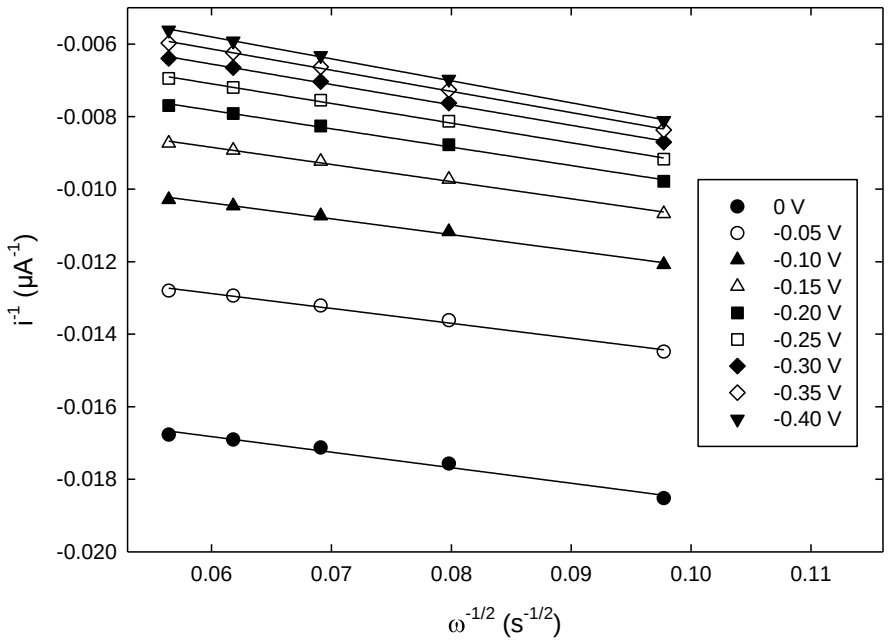


**Figure 6.** Koutecky-Levich plots at different potentials using data extracted from Fig. 5.

All the resulting curves were successfully fitted using a linear regression and the intercepts provided the values of the kinetic-limited current contribution $i_k$. Finally ln $i_k$ was plotted as a function of the potential (Figure 7). From this latter graph, the cathodic transfer coefficient β was obtained from the expression of the charge transfer rate constant k (Equation (2)):

$$k = k° \exp\left(-\frac{\beta F}{RT}(E - E°')\right) \qquad (2)$$

where k° (cm $s^{-1}$) is the intrinsic charge transfer rate constant, R is the gas constant (8.31 J $mol^{-1}$ $K^{-1}$), and E°' is the apparent standard potential (V).

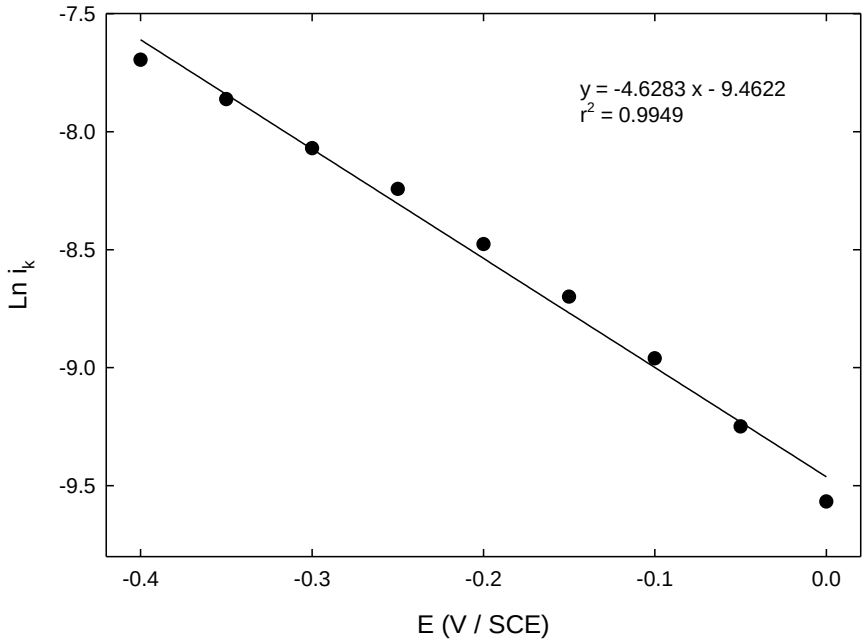


**Figure 7.** Variation of the kinetics-limited current Ln $i_k$ corresponding to $Fe(CN)_6^{3-}$ reduction on GC-NHOH$^{300\ s}$ as a function of the applied potential.

A similar treatment was applied to GC-NHOH prepared using shorter grafting times and to all the corresponding GC-$NO_2^{grafting\ time}$ and GC-$NH_2^{grafting\ time}$. In order to get more information on the influence of the aromatic substituent, graftings were also performed using an unsubstituted diazonium salt, namely phenyldiazonium, and the corresponding interfaces GC-Ph$^{grafting\ time}$ studied as the other three. For the sake of comparison, all the obtained β values were normalized with respect to $\beta_{GC}$, i.e. the β value experimentally determined for $Fe(CN)_6^{3-}$ on bare GC (ca. 0.45). All these results are summarized on Figure 8A and Table 1.

Clearly, the interface bearing $NO_2$ groups exhibited the most blocking behavior compared to the interfaces with NHOH or $NH_2$, as the $\beta/\beta_{GC}$ ratio was found systematically lower in the former case for a given grafting time (Figure 8A and Table 1). Also, the comparison between GC-$NO_2^{grafting\ time}$ and GC-Ph$^{grafting\ time}$ evidenced the respective contribution of $NO_2$ groups and the aromatic skeleton on the kinetics lowering: except for short grafting times (ca. between 1 and 10 s) which produce very thin films, the $\beta/\beta_{GC}$ ratio was always slightly lower when operating on the $NO_2$-bearing interface. It is worth noting that for GC-$NO_2^{grafting\ time}$, the $\beta/\beta_{GC}$ ratio decreased as soon as 1 s grafting ($\beta/\beta_{GC}$ = 0.70) down to a limit value ca. 0.33 for 30 s grafting or longer time. If the first, decreasing trend is logical since one may expect the thicker the film, the lower the kinetics, the almost absence of evident link between film thickness and $\beta/\beta_{GC}$ value for grafting time higher than 30 s is more surprising, especially taking into account that it has been reported in the literature that diazonium films growth usually continues up to 300 s grafting [25].

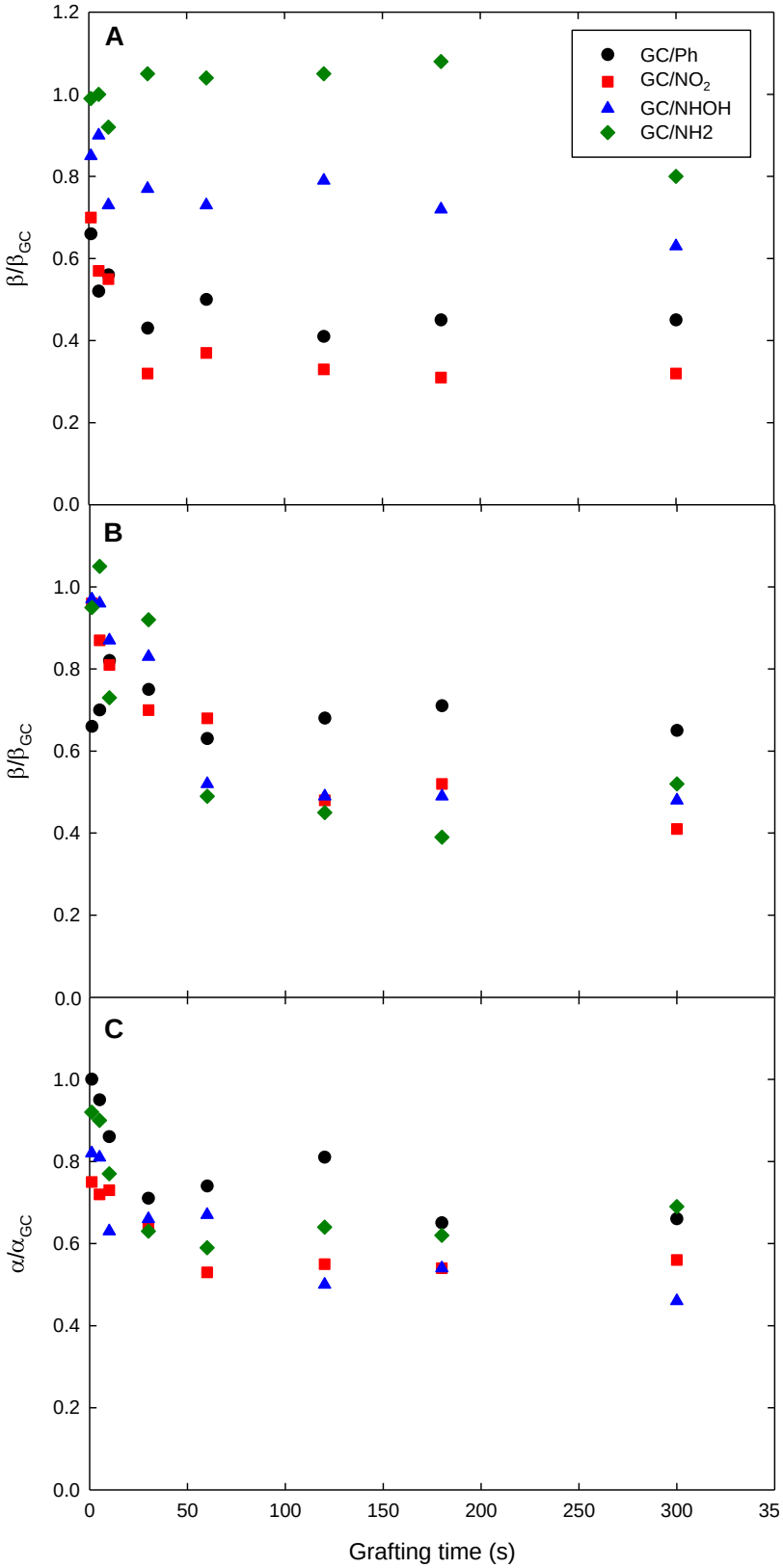


**Figure 8.** Cathodic (β) and anodic (α) transfer coefficients as a function of diazonium grafting time for: (A) $Fe(CN)_6^{3-}$; (B) $Ru(NH_3)_6^{3+}$; (C) FcMeOH. (Black circle) GC/-Ph; (red square) GC-$NO_2$; (blue triangle) GC-NHOH; (green diamond) GC-$NH_2$. All the values are normalized with respect to that found on unmodified GC.

**Table 1.** Values of the cathodic transfer coefficients ratio $\beta/\beta_{GC}$ of $Fe(CN)_6^{3-}$ obtained by the Koutecky-Levich and Tafel methods as a function of diazonium grafting time for different substituted or unsubstituted compounds from steady-state voltammograms recorded in 0.1 M $KPF_6$ (pH 3.5) containing 5 mM $Fe(CN)_6^{3-}$. $\beta_{GC}$ = 0.45 ± 0.04 (calculated using same methods on unmodified GC electrode).

| $t_{grafting}$ (s) | GC-$NO_2$ | GC-NHOH | GC-$NH_2$ | GC-Ph |
|---|---|---|---|---|
| 1 | 0.70 ± 0.02 | 0.85 ± 0.01 | 0.99 ± 0.14 | 0.66 ± 0.04 |
| 5 | 0.57 ± 0.08 | 0.90 ± 0.11 | 1.00 ± 0.05 | 0.52 ± 0.08 |
| 10 | 0.55 ± 0.12 | 0.73 ± 0.10 | 0.92 ± 0.02 | 0.56 ± 0.06 |
| 30 | 0.32 ± 0.10 | 0.77 ± 0.08 | 1.05 ± 0.04 | 0.43 ± 0.03 |
| 60 | 0.37 ± 0.04 | 0.73 ± 0.09 | 1.04 ± 0.08 | 0.50 ± 0.06 |
| 120 | 0.33 ± 0.05 | 0.79 ± 0.04 | 1.05 ± 0.03 | 0.41 ± 0.04 |
| 180 | 0.31 ± 0.04 | 0.72 ± 0.06 | 1.08 ± 0.08 | 0.45 ± 0.09 |
| 300 | 0.32 ± 0.08 | 0.63 ± 0.07 | 0.80 ± 0.10 | 0.45 ± 0.05 |

This latter observation suggests that for thick films, $Fe(CN)_6^{3-}$ mass transport up to the electrode surface and subsequent charge transfer mainly occurs via pinholes or defects that are present into the organic film, and the density of which does not evolve while increasing the film thickness. This is consistent with the fact that 30 s is generally considered as the average time needed to produce a complete monolayer onto the electrode surface when an overpotential sufficient enough is applied [14]. On GC-$NHOH^{grafting\ time}$, the $\beta/\beta_{GC}$ ratio slowly decreased while increasing the grafting time without reaching a limit value. Keeping in mind that at such a pH value (ca. 3.5) NHOH groups are under their protonated form, one may assume the barrier effect afforded by growing organic layer is counterbalanced by the favorable electrostatic interaction between the positively charged film and $Fe(CN)_6^{3-}$. On GC-$NH_2^{grafting\ time}$, the $\beta/\beta_{GC}$ ratio appeared to be barely affected by the presence of the organic film, except for the latest value corresponding to a 300 s grafting which was slightly lower, although in the limit of the calculated uncertainties. In a similar trend compared to GC-$NHOH^{grafting\ time}$, one has to consider the amino groups to be under their $NH_3^+$ form which is electrostatically more favorable to $Fe(CN)_6^{3-}$ than protonated hydroxylamino groups. Moreover, an additional hypothesis to account for these results would be to consider that GC-$NH_2$ affords a less sterically hindered film than GC-NHOH, which may thus favor $Fe(CN)_6^{3-}$ approach to the electrode surface via the pinholes. Finally, it has to be noticed that, for a given grafting time, the $\beta/\beta_{GC}$ ratio was systematically found to increase following the trend GC-$NO_2$ < GC-NHOH < GC-$NH_2$. This latter observation is consistent with the fact that nitro groups exhibit strong unfavorable electrostatic interaction with the anionic $Fe(CN)_6^{3-}$ redox probe, while NHOH and $NH_2$ under their protonated form favor this latter interaction. Thus, in this case, the aromatic substituent plays a key role in the electrochemical kinetic since it is capable of diminish the barrier effect of the film.

The same experiments were performed using hexammineruthenium(III) $Ru(NH_3)_6^{3+}$ as the redox probe. The results corresponding to the evolution of the $\beta/\beta_{GC}$ ratio as a function of grafting time for the 4 different diazonium-functionalized interfaces are summarized on Figure 8B and Table 2.

**Table 2.** Values of the cathodic transfer coefficients ratio $\beta/\beta_{GC}$ of $Ru(NH_3)_6^{3+}$ obtained by the Koutecky-Levich and Tafel methods as a function of diazonium grafting time for different substituted or unsubstituted compounds from steady-state voltammograms recorded in 0.1 M $KPF_6$ (pH 3.5) containing 5 mM $Ru(NH_3)_6^{3+}$. $\beta_{GC} = 0.53 \pm 0.04$ (calculated using same methods on unmodified GC electrode).

| $t_{grafting}$ (s) | GC-$NO_2$ | GC-NHOH | GC-$NH_2$ | GC-Ph |
|---|---|---|---|---|
| 1 | 0.96 ± 0.14 | 0.97 ± 0.04 | 0.95 ± 0.10 | 0.66 ± 0.11 |
| 5 | 0.87 ± 0.06 | 0.96 ± 0.12 | 1.05 ± 0.08 | 0.70 ± 0.07 |
| 10 | 0.81 ± 0.10 | 0.87 ± 0.11 | 0.73 ± 0.03 | 0.82 ± 0.06 |
| 30 | 0.77 ± 0.11 | 0.83 ± 0.05 | 0.92 ± 0.08 | 0.75 ± 0.10 |
| 60 | 0.68 ± 0.09 | 0.52 ± 0.10 | 0.49 ± 0.13 | 0.63 ± 0.08 |
| 120 | 0.48 ± 0.12 | 0.49 ± 0.07 | 0.45 ± 0.12 | 0.68 ± 0.14 |
| 180 | 0.52 ± 0.08 | 0.49 ± 0.10 | 0.39 ± 0.10 | 0.71 ± 0.15 |
| 300 | 0.41 ± 0.06 | 0.48 ± 0.15 | 0.52 ± 0.11 | 0.65 ± 0.13 |

The trends observed in this case were drastically different from that found for $Fe(CN)_6^{3-}$. In particular, no important difference was noticed at a given time between the three different substituents, namely $NO_2$, NHOH and $NH_2$, thus suggesting that the nature of these latter was almost without effect on the value of the $\beta/\beta_{GC}$ ratio. This is consistent with the fact that $Ru(NH_3)_6^{3+}$ reduction proceeds via an outer-sphere mechanism, which makes it much less sensitive to surface modification than $Fe(CN)_6^{3-}$. However, and independently on its own nature, the presence of the substituent in the layer has an influence on the $\beta/\beta_{GC}$ ratio. This can be seen by comparing the evolution of the $\beta/\beta_{GC}$ ratio for any of the three substituents to that recorded on GC-Ph, which was barely constant whatever the grafting time: at short grafting time, i.e. up to 30 s, the $\beta/\beta_{GC}$ ratio were higher for substituted films compared to the unsubstituted one, whereas at grafting time longer than 30 s the trend was reversed. Thus, for short grafting times, which produce submonolayer films, steric hindrance induced by the presence of the substituent seems to be overriding compared to any other effect, considering aromatics bearing substituents lead to less dense, and consequently less blocking films than unsubstituted moieties. For grafting time longer than 30 s, all three substituents clearly exhibit a negative effect on the $\beta/\beta_{GC}$ ratio. Once again, this effect seemed to be independent on their own nature since at a given time, the obtained values were comparable whatever the substituent. Thus, the cationic nature of the hydroxylamino and amino groups at pH 3.5 cannot be invoked to explain such a trend, or at least, it does not afford the main contribution to the whole effect.

Finally, a third redox probe was studied, namely ferrocenemethanol FcMeOH, which reduces via an outer-sphere process and is a neutral compound. It may thus be assumed to remain unaffected by electrostatic effects. The results corresponding to this latter probe are depicted on Figure 8C and Table 3.

For all four interfaces, a comparable trend was observed with a strong decrease in the $\alpha/\alpha_{GC}$ ratio for grafting times up to 30 s and then, no further evolution of this latter values was noticed for grafting time longer than 30 s. This result which shows that for this electrostatic-free probe the functionalized interfaces undergo the "classical" barrier effects supports well the hypothesis of electrostatic effects in

the case of positively or negatively charged redox probe such as hexammineruthenium(III) and ferricyanide, respectively.

**Table 3.** Values of the anodic transfer coefficients ratio $\alpha/\alpha_{GC}$ of FcMeOH obtained by the Koutecky-Levich and Tafel methods as a function of diazonium grafting time for different substituted or unsubstituted compounds from steady-state voltammograms recorded in 0.1 M $KPF_6$ (pH 3.5) containing 5 mM FcMeOH. $\alpha_{GC}$ = 0.52 ± 0.05 (calculated using same methods on unmodified GC electrode).

| $t_{grafting}$ (s) | GC-$NO_2$ | GC-NHOH | GC-$NH_2$ | GC-Ph |
|---|---|---|---|---|
| 1 | 0.75 ± 0.04 | 0.82 ± 0.07 | 0.92 ± 0.04 | 1.00 ± 0.04 |
| 5 | 0.72 ± 0.08 | 0.81 ± 0.08 | 0.90 ± 0.02 | 0.95 ± 0.06 |
| 10 | 0.73 ± 0.09 | 0.63 ± 0.05 | 0.77 ± 0.10 | 0.86 ± 0.05 |
| 30 | 0.64 ± 0.10 | 0.66 ± 0.06 | 0.63 ± 0.06 | 0.71 ± 0.08 |
| 60 | 0.53 ± 0.10 | 0.67 ± 0.03 | 0.59 ± 0.05 | 0.74 ± 0.10 |
| 120 | 0.55 ± 0.03 | 0.50 ± 0.04 | 0.64 ± 0.08 | 0.81 ± 0.09 |
| 180 | 0.54 ± 0.04 | 0.54 ± 0.04 | 0.62 ± 0.10 | 0.65 ± 0.11 |
| 300 | 0.56 ± 0.06 | 0.46 ± 0.06 | 0.69 ± 0.05 | 0.66 ± 0.10 |

## 4. CONCLUSION

The kinetics of three redox probes, namely ferricyanide, hexammineruthenium(III) and ferrocenemethanol were studied on diazonium functionalized GC electrodes bearing either $NO_2$, NHOH or $NH_2$ groups or no substituent and prepared by constant potential electrolysis for duration ranging between 1 and 300 s in order to vary films thickness. In all the cases, experimental results showed the electron transfer throughout the films to occur mainly via pinholes, except for short grafting times which correspond to submonolayer films. The substituents borne by the aromatic skeleton proved to have a strong influence on the kinetics of the redox probes by means of electrostatic effects that favor or disfavor the approach of the probes. As expected, ferricyanide, the reduction process of which is known to proceed via an inner-sphere mechanism was the most affected by substituent changes in the films. In this case and for a given grafting time, the $\beta/\beta_{GC}$ ratio was found to increase following the trend GC-$NO_2$ < GC-NHOH < GC-$NH_2$. All these results help providing a better understanding of electron transfer mechanism throughout diazonium insulating films.

## References

1. V. M. Mirsky, *TrAC, Trends Anal. Chem.*, 21 (2002) 439.
2. M. D. Imisides, R. John, Peter J. and G. G. Wallace, *Electroanalysis*, 3 (1991) 879.

3. M. Xu, J. Wang and F. Zhou, *Curr. Top. Electrochem.*, 11 (2006) 57.
4. D. Bélanger and J. Pinson, *Chem. Soc. Rev.*, 40 (2011) 3995.
5. R. L. McCreery, *Chem. Rev.*, 108 (2008) 2646.
6. S. Mahouche-Chergui, S. Gam-Derouich, C. Mangeney and M. M. Chehimi, *Chem. Soc. Rev.*, 40 (2011) 4143.
7. J. T. Abrahamson, C. Song, J. H. Hu, J. M. Forman, S. G. Mahajan, N. Nair, W. Choi, E.-J. Lee and M. S. Strano, *Chem. Mater.*, 23 (2011) 4557.
8. D. J. Bates, C. M. Elliott and A. L. Prieto, *Chem. Mater.*, 26 (2014) 5514.
9. W. Richard, D. Evrard and P. Gros, *Electroanalysis*, 26 (2014) 1390.
10. J. A. Rather, A. J. Al Harthi, E. A. Khudaish, A. Qurashi, A. Munam and P. Kannan, *Anal. Methods*, 8 (2016) 5690.
11. D.-J. Chung, K.-C. Kim and S.-H. Choi, *Appl. Surf. Sci.*, 257 (2011) 9390.
12. S. M. Khor, G. Liu, J. R. Peterson, S. G. Iyengar and J. J. Gooding, *Electroanalysis*, 23 (2011) 1797.
13. R. T. Jane, E. Gaudemer and R. Lomoth, *J. Mater. Chem. C*, 3 (2015) 10023.
14. D. Evrard, F. Lambert, C. Policar, V. Balland and B. Limoges, *Chem. Eur. J.*, 14 (2008) 9286.
15. S. Descroix, G. Hallais, C. Lagrost and J. Pinson, *Electrochim. Acta*, 106 (2013) 172.
16. C. Jiang, S. M. Silva, S. Fan, Y. Wu, M. T. Alam, G. Liu and J. J. Gooding, *J. Electroanal. Chem.*, 785 (2017) 265.
17. R. Sharma, J. H. Baik, C. J. Perera and M. S. Strano, *Nano Lett.*, 10 (2010) 398.
18. T. Menanteau, E. Levillain and T. Breton, *Langmuir*, 30 (2014) 7913.
19. P. A. Brooksby and A. J. Downard, *Langmuir*, 21 (2005) 1672.
20. V. Vijaikanth, J.-F. Capon, F. Gloaguen, P. Schollhammer and J. Talarmin, *Electrochem. Commun.*, 7 (2005) 427.
21. X.-Y. Fan, R. Nouchi, L.-C. Yin and K. Tanigaki, *Nanotechnology*, 21 (2010) 475208/1.
22. C. Saby, B. Ortiz, G. Y. Champagne and D. Belanger, *Langmuir*, 13 (1997) 6805.
23. M. Delamar, G. Desarmot, O. Fagebaume, R. Hitmi, J. Pinson and J. M. Saveant, *Carbon*, 35 (1997) 801.
24. A. J. Downard, *Langmuir*, 16 (2000) 9680.
25. P. A. Brooksby and A. J. Downard, *Langmuir*, 20 (2004) 5038.
26. J. Pinson and F. Podvorica, *Chem. Soc. Rev.*, 34 (2005) 429.
27. J. Haccoun, C. Vautrin-Ul, A. Chausse and A. Adenier, *Prog. Org. Coat.*, 63 (2008) 18.
28. W. Richard, D. Evrard and P. Gros, *J. Electroanal. Chem.*, 685 (2012) 109.
29. K. K. Cline, L. Baxter, D. Lockwood, R. Saylor and A. Stalzer, *J. Electroanal. Chem.*, 633 (2009) 283.
30. P. Allongue, M. Delamar, B. Desbat, O. Fagebaume, R. Hitmi, J. Pinson and J.-M. Saveant, *J. Am. Chem. Soc.*, 119 (1997) 201.
31. W. Richard, D. Evrard, B. Busson, C. Humbert, L. Dalstein, A. Tadjeddine and P. Gros, *Electrochim. Acta*, 283 (2018) 1640.
32. M. Ceccato, L. T. Nielsen, J. Iruthayaraj, M. Hinge, S. U. Pedersen and K. Daasbjerg, *Langmuir*, 26 (2010) 10812.
33. A. J. Downard and M. J. Prince, *Langmuir*, 17 (2001) 5581.
34. E. Gervais, Y. Aceta, P. Gros and D. Evrard, *Electrochim. Acta*, 261 (2018) 346.
35. S. Baranton and D. Belanger, *J. Phys. Chem. B*, 109 (2005) 24401.
36. S. S. C. Yu and A. J. Downard, *e-J. Surf. Sci. Nanotech.*, 3 (2005) 294.
37. A. Omrani, A. A. Rostami, N. Yazdizadeh and M. Khoshroo, *Chem. Phys. Lett.*, 539-540 (2012) 107.
38. V. Branzoi, F. Branzoi, M. Raicopol and L. Pilan, *Rev. Chim.*, 62 (2011) 436.
39. P. Chen and R. L. McCreery, *Anal. Chem.*, 68 (1996) 3958.
40. S. Schauff, M. Ciorca, A. Laforgue and D. Bélanger, *Electroanalysis*, 21 (2009) 1499.

41. A. Badia, R. Back and R. B. Lennox, *Angew. Chem. Int. Ed.*, 33 (1994) 2332.
42. J. Koutecky, *Chem. Listy Vedu Prum.*, 47 (1953) 1758.
43. J. P. Diard, B. Le Gorrec, C. Montella and C. Hecker, *Surface Technology*, 15 (1982) 363.